Title: Catalytic Enantioselective Pyridine *N*-Oxidation

Authors: Sheng-Ying Hsieh, Yu Tang, Simone Crotti, Elizabeth A. Stone and Scott J. Miller*.

Affiliations: Department of Chemistry, Yale University, New Haven, Connecticut 06520-8107, United States

*Correspondence to: scott.miller@yale.edu

Abstract: The catalytic, enantioselective *N*-oxidation of substituted pyridines is described. The approach is predicated on a biomolecule-inspired catalytic cycle wherein high levels of asymmetric induction are provided by aspartic acid-containing peptides as the aspartyl side chain shuttles between free acid and peracid forms. Desymmetrizations of bis(pyridine) substrates bearing a remote pro-stereogenic center are demonstrated, presenting a new entry into chiral pyridine frameworks in a heterocycle-rich molecular environment. Representative functionalizations of the enantioenriched pyridine *N*-oxides further document the utility of this approach. Demonstration of the asymmetric *N*-oxidation in two venerable drug-like scaffolds, Loratadine and Varenicline, show the likely generality of the method for highly variable and distinct chiral environments, while also revealing that the approach is applicable to both pyridines and 1,4-pyrazines.

Substituted pyridines continue to emerge with high frequency in disclosures of biologically active scaffolds (*1–2*). Accordingly, methods for synthesizing differentially substituted analogs are highly coveted (*3–4*). Strategies for constructing pyridine-containing molecules in optically enriched form are generally indirect, given the planarity of the heteroaromatic pyridine *N*-nucleus. Nonetheless, methodologies for achieving "asymmetric", or enantioselective, syntheses of pyridines are essential given the extant and growing number of pyridine-containing chiral molecules now found in drugs and drug candidates (Fig. 1A) (*5–9*).

Please Insert Figure 1

Enantioselective syntheses of pyridines are often predicated on using building blocks containing stereogenic centers (*10*), or appending chiral auxiliaries to the pyridine as a substituent (Fig. 1B, upper schemes) (*11*). Using asymmetric catalysts, chiral pyridines can be accessed through the coupling of chiral fragments (*12–14*) or by performing an asymmetric catalytic reaction on a pyridine with a prochiral element (Fig. 1B, lower scheme) (*15*). Particularly inspiring for the present report, enantioselective *N*-oxidation of tertiary amines (Fig. 1C) was reported by Sharpless in 1983, wherein chiral Ti-based complexes were employed in stoichiometric quantities to affect kinetic resolution of tertiary amines (*16–18*).

We now report herein an alternative, unprecedented catalytic pyridine *N*-oxidation reaction, in which chirality is established *via* remote asymmetric desymmetrization (Fig. 1D). As described below, the chemistry proceeds with high levels of enantio- and chemoselectivity, and we have also achieved derivatizations of the resulting pyridine *N*-oxides (Fig. 1D, right) that add to the versatility of the approach for synthesis. In addition, we have extended this chemistry to intriguing, now-venerable classes of bioactive heterocyclic scaffolds (*vide infra*), which implies generality for this new method.

Our approach required the identification of an appropriate catalytic cycle for pyridine *N*-oxidation, and the design of a substrate-type that would allow us to interrogate enantioselectivity. For the former, we wondered if a recently explored family of biologically inspired oxidation catalysts might suffice. We have shown, for example, that aspartic acid-containing catalysts exhibit significant prowess as enantioselective epoxidation (*19–20*) or asymmetric Baeyer–Villiger (BV) (*21*) catalysts that also exert control over migratory aptitude in BV reactions (Fig. 2A, upper scheme). Furthermore, the peptide sequence can control functional group selectivity, selecting olefins (epoxidation) or ketones (BV), even if both are present within the same molecule, overcoming the specter of cross-reactivity (Fig. 2A, lower scheme) (*22*). Moreover, because these catalysts exhibit high chemoselectivity in the presence of electron-rich heterocycles (*23–24*), we thought they might have the mechanistic generality to serve as selective pyridine *N*-oxidation catalysts, as projected in Fig. 1D. Several other designs of catalytic residues for enantioselective pyridine *N*-oxidation were also considered based on the previous literature (*25–26*).

Please Insert Figure 2

Shown in Fig. 2B is the catalytic cycle we desired to implement for asymmetric pyridine *N*-oxidation of **2** to **3** using Asp-containing catalysts (**1**). Overoxidation to form bis(*N*-oxide) product **4** is also possible, as is a general issue with desymmetrizations wherein double functionalization can occur. Nevertheless, in analogy to epoxidation and BV oxidation, we relied on carbodiimide activation of **1** to chaperone the Asp-containing catalysts to the Asp-based peracid **5**. The desired pyridine *N*-oxidation then completes the catalytic cycle and regenerates **1**. One interesting difference between the presently disclosed pyridine *N*-oxidation and our prior epoxidation and BV catalytic systems is that in this new application, both the substrate **2** and product **3** can serve as transient co-catalysts for the reaction, preventing deleterious rearrangement of the intermediate *O*-acyl urea **6** to the catalytically inactive *N*-acyl urea **7** (*27–28*), possibly through the formation of intermediates like **8**. In our earlier studies, we had deliberately assigned this function to the additive DMAP or DMAP *N*-oxide. Notably, we observed no particular advantage or disadvantage to the incorporation of extra DMAP on the selectivity in the current studies. In any event, we were

pleased to see that with 10 mol% of Boc-Asp-OMe (**1a**) as the catalyst, 63% yield of **2a** could be achieved, albeit in racemic form (Fig. 2C, table, entry 1).

We then turned our attention to the critical question of enantioselectivity. Given nonexistent analogy in the literature for the explicit design of chiral catalysts for pyridine *N*-oxidation, we elected to compare a combinatorial approach to the discovery of a "hit" catalyst to a class of β-turn-biased catalysts we have previously employed for many asymmetric reactions (*29–30*). For the combinatorial approach, we applied the one-bead-one-compound (OBOC) library concept (*31–33*). Application of this approach (described in the supplementary materials) to the desymmetrization of **2a** led to the identification of a number of "hit" catalysts, including **1b** and **1c** (Fig. 2C, scheme). These catalysts delivered **3a** with appreciable enantioselectivity under the conditions of the assay (resin-bound **1b**, 69.5:30.5 enantiomeric ratio (er); resin-bound **1c**, 70:30 er); synthesis and evaluation under homogeneous conditions gave validating results (**1b**, 75:25 er; **1c**, 72:28 er). In parallel, our assessment of β-turn-biased catalysts included a survey of the diastereomers of canonical Boc-Asp-Pro-type tetramers (Fig. 2C, table, entries 2–5) (*30*, *34*), and of these catalysts, **1d** delivered **3a** with 74:26 er. Thus, we elected to pursue catalysts related to **1d** further. Parenthetically, we suspect that any of the three scaffolds depicted in Fig. 2C (scheme) could in principle be optimized for the selective oxidation of **2a** to **3a**.

Accordingly, we then turned to the optimization of catalyst **1d**, exploring simple variations of side chains and stereochemical configurations at each position of the catalyst. Several illustrative and heuristic substitutions are shown in the table of Fig. 2C. First, the monomeric Asp-derived catalyst **1a** noted above delivered the product in racemic form, indicating that some higher-order structure would be necessary for enantioselectivity (Fig. 2C, table, entry 1). Furthermore, the survey of the stereochemical disposition of each residue in the β-turn-biased sequence (entries 2–5) revealed that Boc-D-Asp-D-Pro-Acpc-Phe-OMe (**1d**) was indeed optimal, delivering the 74:26 er, while other diastereomers gave lower selectivity. Deuterated chloroform also emerged as the preferred solvent with catalyst **1d** in a preliminary survey (entries 6–7). Variation of the *i*+2 residue generally led to catalysts with lower selectivity (entries 8–9); yet, variation of substituents to the *N*-terminal side of the peptide sequence led to promising improvements. An *N*-terminal *tert*-

butylurea substituent (**1j**, entry 10) resulted in observation of nearly 80:20 er. Addition of a fifth amino acid residue to the *N*-terminal side gave further enhancement of er (entries 11–17). Of these catalysts, peptide **1n** with a Boc-D-phenylglycine (Boc-D-Phg, entry 15) *N*-terminal residue delivered **3a** with an 86:14 er. Accordingly, we elected to examine this catalyst further with a variety of reaction conditions and for studies of substrate scope.

Variations of the reaction parameters impacted the enantioselectivity, but none more profound than the nature of the 6- and 6′-positions of **2**. Thus, when **2b** was employed, with a methyl group at the 6- and 6′-positions, we observed an increase in the er such that **3b** was produced with 92:8 er, and in 71% isolated yield (Fig. 2D, entry 1). Moreover, we discovered that there was a degree of secondary kinetic resolution in the overoxidation of **3b** (to give **4b**) that led to further er enhancement (entries 2–4). Indeed, **3b** was generated with >98:2 er when 1.6 equiv of DIC was employed, albeit with a small sacrifice in yield (55% yield). With this level of enantioselectivity, we turned our attention to the scope and limitations for this new asymmetric process.

Our explorations of substrates led to the identification of a number of excellent substrates, as well as some that did not work as well. Under optimized conditions (1.5 equiv oxidant, 0.2 M in substrate, 4 °C), **3a** was isolated in 75% yield with 87:13 er (Fig. 3A). In addition, quite a few excellent substrates emerged with 6,6'-disubstitution. For example, **3b** was isolated in 76% yield with 97:3 er. *iso*-Propyl-bearing product **3c** was also obtained with high er (71% yield, 99:1 er), as was the *tert*-butyl substituted compound **3d** (70% yield, 98.5:1.5 er), albeit requiring a 48 h reaction time in this case. Similarly, the cyclohexyl-bearing substrate **2e** was converted to **3e** with 99:1 er (69% isolated yield). Aryl-substituted pyridines were also well-tolerated by catalyst **1n**, as illustrated by the isolations of **3f** (78% yield, 98:2 er), **3g** (78% yield, 99:1 er), **3h** (74 % yield, 98:2 er) and **3i** (79% yield, 96:4 er). Some other more exotic substituents were also promising, as bis(quinoline) **3j** was isolated in 79% yield with 97:3 er under these conditions. 6,6′-Bismethoxy-substitution was less tolerated, although **3k** was still isolated with 88:12 er and in 67% yield. Altering the position of the pyridyl substituent to 5,5′-dimethylation led to a product with somewhat lower selectivity, as **3l** was isolated with 87:13 er and 65% yield. The absolute

configuration of *N*-oxide 3l was determined by single crystal X-ray diffraction, which enabled the assignment of the remaining substrates by analogy.

Please Insert Figure 3

On the other hand, Fig. 3B depicts several substrates that do not work as well with peptide **1n**, including substitution at the 2-position of the pyridine (**3m**) or when the pyridyl moieties are bridged at the 4-positions (**3n**). These two cases afforded products that were nearly racemic with catalyst **1n**. In addition, compounds related to **3** generally exhibited higher selectivity when the bridging amide group was a secondary pivaloyl amide. When the free *N*-H group was replaced with *N*-Me (**3o**), selectivity was greatly diminished (54:46 er), suggesting that the secondary amide may play a mechanistic role as a hydrogen bond donor. When the pivaloyl group was converted to benzoyl (**3p**) or acetyl (**3q**), selectivity was partially restored (84:16 er and 72:28 er, respectively). It is certainly possible that re-optimization with another catalyst from our library might address these classes in a more selective manner.

While we do not yet know the basis of asymmetric induction in the highly selective variants of these reactions, we are in a position to offer some speculation in analogy to previous studies. In this spirit, the ensemble shown in Fig. 3C presents a schematic drawing in which the activated aspartic peracid catalytic intermediate may interact with the substrate in a manner that is consistent with the identity of the major enantiomer in the (*S*)-configuration that we observe. This model is predicated on well-precedented conformational analyses for Pro-Acpc peptides (*30, 35*), and accommodates the SAR derivable from Fig. 3B. In this speculative transition state, the peptide adopts a type II′ β-turn conformation in the reactive complex. Hydrogen bonding interactions are envisioned to contribute to catalyst-substrate organization.

The optically enriched pyridine *N*-oxides emerging from this study also provide a platform for the synthesis of chiral pyridine-containing scaffolds, as demonstrated in Fig. 4. For example, Ph-substituted pyridine *N*-oxide **3f** was permuted to aminopyridine **9**, aryloxypyridine **10**, and

thioether variant **11** under established PyBroP®-based substitution conditions (Fig. 4A) (*36–37*). Parenthetically, the desymmetrized unsubstituted pyridine *N*-oxide **3a** may also be regioselectively diversified. For example, using recrystallized material of **3a** (91:9 er), amination delivered **12** in a 15:1 ratio of 2/6 positional regioisomers, while sulfonamidation (**13**) occurred in a >19:1 ratio of 6/2 positional regioisomers (Fig. 4B).

Please Insert Figure 4

To address the question of whether our approach might be applicable generally, and in genuinely different classes of substrates, we conclude with two exotic and demanding applications in unambiguously drug-like scaffolds. Loratadine (*38–39*), the active ingredient in the allergy medicine Claritin®, exhibits unusual stereochemical properties. For example, while Loratadine itself does not exhibit stable enantiomers due to rapid conformational interconversion, compounds like **14** can be isolated with optically purity due to high barriers to racemization of the helically chiral enantiomers (Fig. 4C) (*40*). Thus, we wondered whether or not catalytic, enantioselective pyridine *N*-oxidation of Loratadine derivative **15** could be subjected to dynamic kinetic resolution. Notably, catalyst **1d** afforded **16** in 45% yield with 95:5 er (Fig. 4C). Pyridine *N*-oxidation is preferred, although we also observed 28% conversion to the corresponding epoxide under these conditions, as assayed by LC/MS. This result highlights the applicability of this chemistry beyond desymmetrizations. Moreover, we demonstrated that a scaffold related to Varenicline (*41–42*) may undergo desymmetrization, such that **17** was converted to **18** with catalyst **1d** in 61% yield and with 95.5:4.5 er (Fig. 4D). This last result suggests the present approach may have generality with respect to other, enantio- and site-selective heteroarene *N*-oxidations.

In conclusion, we have described a fundamentally new enantioselective transformation: the catalytic, asymmetric *N*-oxidation of pyridines employing aspartic acid-derived peracid catalysis. This chemistry not only extends the general utility of this catalytic cycle beyond epoxidation and Baeyer-Villiger oxidations, but also provides strategic access to optically enriched heterocycles in a class of substrates fertile for studies of bioactivity. With efficiency demonstrated for a range of

desymmetrizations, heterocycles, and enantioselective derivatization of drug-like scaffolds, we anticipate this approach will be of interest and use in fundamental and applied studies in both process-oriented and discovery-oriented synthetic chemistry settings.

References and Notes:

(*1*) R. D. Taylor, M. MacCoss, A. D. G. Lawson, Rings in drugs. *J. Med. Chem.* ***57***, 5845–5859 (2014).

(*2*) E. Vitaku, D. T. Smith, J. T. Njardarson, Analysis of the structural diversity, substitution patterns, and frequency of nitrogen heterocycles among U.S. FDA approved pharmaceuticals. *J. Med. Chem.* ***57***, 10257–10274 (2014).

(*3*) G. D. Henry, *De novo* synthesis of substituted pyridines. *Tetrahedron* ***60***, 6043–6061 (2004).

(*4*) M. D. Hill, Recent strategies for the synthesis of pyridine derivatives. *Chem. Eur. J.* ***16***, 12052–12062 (2010).

(*5*) A. J. Roecker, S. P. Mercer, J. D. Schreier, C. D. Cox, M. E. Fraley, J. T. Steen, W. Lemaire, J. G. Bruno, C. M. Harrell, S. L. Garson, A. L. Gotter, S. V. Fox, J. Stevens, P. L. Tannenbaum, T. Prueksaritanont, T. D. Cabalu, D. Cui, J. Stellabott, G. D. Hartman, S. D. Young, C. J. Winrow, J. J. Renger, P. J. Coleman, Discovery of 5″-chloro-*N*-[(5,6-dimethoxypyridin-2-yl)methyl]-2,2′:5′,3″-terpyridine-3′-carboxamide (MK-1064): a selective orexin 2 receptor antagonist (2-SORA) for the treatment of insomnia, *ChemMedChem* ***9***, 311–322 (2014).

(*6*) J. Ding, D. G. Hall, Concise synthesis and antimalarial activity of all four mefloquine stereoisomers using a highly enantioselective catalytic borylative alkene isomerization. *Angew. Chem. Int. Ed.* ***52***, 8069–8073 (2013).

(*7*) E. J. Rastelli, D. M. Coltart, A concise and highly enantioselective total synthesis of (+)-anti- and (−)-syn-mefloquine hydrochloride: definitive absolute stereochemical assignment of the mefloquines. *Angew. Chem. Int. Ed.* ***54***, 14070–14074 (2015).

(*8*) A. H. Parton, M. H. Ali, D. C. Brookings, J. A. Brown, D. J. Ford, R. J. Franklin, B. J. Langham, J. C. Neuss, J. R. Quincey, Quinoline and quinoxaline derivatives as kinase inhibitors. WO2012/032334 (2012).

(*9*) D. C. Brookings, "8.15 - The discovery and development of seletalisib: a potent and selective PI3Kδ inhibitor for inflammatory diseases" in *Comprehensive Medicinal Chemistry III*, S. Chackalamannil, D. Rotella, S. E. Ward, Eds. (Elsevier, Oxford, 2017) pp. 366–407.

(*10*) C. Tanyeli, İ. M Akhmedov, M. Işık, Synthesis of various camphor-based chiral pyridine derivatives. *Tetrahedron Lett.* ***45***, 5799–5801 (2004).

(*11*) S. D. Kuduk, R. M. DiPardo, R. K. Chang, C. Ng, M. G. Bock, Reversal of diastereoselection in the addition of Grignard reagents to chiral 2-pyridyl *tert*-butyl (Ellman) sulfinimines. *Tetrahedron Lett.* ***45***, 6641–6643 (2004).

(*12*) R. S. J. Proctor, H. J. Davis, R. J. Phipps, Catalytic enantioselective Minisci-type addition to heteroarenes. *Science* ***360***, 419–422 (2018).

(*13*) Y. Yin, Y. Dai, H. Jia, J. Li, L. Bu, B. Qiao, X. Zhao, Z. Jiang, Conjugate addition–enantioselective protonation of *N*-aryl glycines to α-branched 2-vinylazaarenes via cooperative photoredox and asymmetric catalysis" *J. Am. Chem. Soc.* ***140***, 6083–6087 (2018).

(*14*) K. Cao, S. M. Tan, R. Lee, S. Yang, H. Jia, X. Zhao, B. Qiao, Z. Jiang, Catalytic enantioselective addition of prochiral radicals to vinylpyridines" *J. Am. Chem. Soc.* ***141***, 5437–5443 (2019).

(*15*) X. Tao, W. Li, X. Ma, X. Li, W. Fan, X. Xie, T. Ayad, V. Ratovelomanana-Vidal, Z. Zhang, Ruthenium-catalyzed enantioselective hydrogenation of aryl-pyridyl ketones. *J. Org. Chem.* ***77***, 612–616 (2012).

(*16*) S. Miyano, L. D. L. Lu, S. M. Viti, K. B. Sharpless, Kinetic resolution of racemic β-hydroxy amines by enantioselective *N*-oxide formation. *J. Org. Chem.* ***48***, 3608–3611 (1983).

(*17*) S. Miyano, L. D. L. Lu, S. M. Viti, K. B. Sharpless, Kinetic resolution of racemic β-hydroxy amines by enantioselective *N*-oxide formation. *J. Org. Chem.* ***50***, 4350–4360 (1985).

(*18*) S. Bhadra, H. Yamamoto, Catalytic asymmetric synthesis of *N*-chiral amine oxides. *Angew. Chem. Int. Ed.* ***55***, 13043–13046 (2016).

(*19*) G. Peris, C. E. Jakobsche, S. J. Miller, Aspartate-catalyzed asymmetric epoxidation reactions. *J. Am. Chem. Soc.* ***129***, 8710–8711 (2007).

(*20*) P. A. Lichtor, S. J. Miller, Combinatorial evolution of site- and enantioselective catalysts for polyene epoxidation. *Nat. Chem*. ***4***, 990–995 (2012).

(*21*) D. K. Romney, S. M. Colvin, S. J. Miller, Catalyst control over regio- and enantioselectivity in Baeyer–Villiger oxidations of functionalized ketones. *J. Am. Chem. Soc*. ***136***, 14019–14022 (2014).

(*22*) J. S. Alford, N. C. Abascal, C. R. Shugrue, S. M. Colvin, D. K. Romney, S. J. Miller, Aspartyl oxidation catalysts that dial in functional group selectivity, along with regio- and stereoselectivity. *ACS Cent. Sci.* ***2***, 733–739 (2016).

(*23*) F. Kolundzic, M. N. Noshi, M. Tjandra, M. Movassaghi, S. J. Miller, Chemoselective and enantioselective oxidation of indoles employing aspartyl peptide catalysts. *J. Am. Chem. Soc.* ***133***, 9104–9111 (2011).

(*24*) E. V. Mercado-Marin, P. Garcia-Reynaga, S. Romminger, E. F. Pimenta, D. K. Romney, M. W. Lodewyk, D. E. Williams, R. J. Andersen, S. J. Miller, D. J. Tantillo, R. G. S. Berlinck, R. Sarpong, Total synthesis and isolation of citrinalin and cyclopiamine congeners. *Nature* ***509***, 318–324 (2014).

(*25*) D. Limnios, C. G. Kokotos, 2,2,2-Trifluoroacetophenone as an organocatalyst for the oxidation of tertiary amines and azines to *N*-oxides. *Chem. Eur. J.* ***20***, 559–563 (2014).

(*26*) R. M. B. Dyer, P. L. Hahn, M. K. Hilinski, Selective heteroaryl *N*-oxidation of amine-containing molecules. *Org. Lett*. ***20***, 2011–2014 (2018).

(*27*) J. Rebek, R. McCready, S. Wolf, A. Mossman, New oxidizing agents from the dehydration of hydrogen peroxide. *J. Org. Chem.* ***44***, 1485–1493 (1979).

(*28*) F. D. Greene, J. Kazan, Preparation of diacyl peroxides with *N,N′*-dicyclohexylcarbodiimide. *J. Org. Chem.* ***28***, 2168–2171 (1963).

(*29*) A. J. Metrano, S. J. Miller, Peptide-based catalysts reach the outer sphere through remote desymmetrization and atroposelectivity. *Acc. Chem. Res.* ***52***, 199–215 (2019).

(*30*) A. J. Metrano, N. C. Abascal, B. Q. Mercado, E. K. Paulson, A. E. Hurtley, S. J. Miller, Diversity of secondary structure in catalytic peptides with β-turn-biased sequences. *J. Am. Chem. Soc.* ***139***, 492–516 (2017).

(*31*) K. S. Lam, M. Lebl, V. Krchnák, The "one-bead-one-compound" combinatorial library method. *Chem. Rev.* ***97***, 411–448 (1997).

(*32*) S. J. Miller, In search of peptide-based catalysts for asymmetric organic synthesis. *Acc. Chem. Res.* ***37***, 601–610 (2004).

(*33*) J. D. Revell, H. Wennemers, Peptidic catalysts developed by combinatorial screening methods. *Curr. Opin. Chem. Biol.* ***11***, 269–278 (2007).

(*34*) T. S. Haque, J. C. Little, S. H. Gellman, Stereochemical requirements for β-hairpin formation: model studies with four-residue peptides and depsipeptides. *J. Am. Chem. Soc.* ***118***, 6975–6985 (1996).

(*35*) A. E. Hurtley, E. A. Stone, A. J. Metrano, S. J. Miller, Desymmetrization of diarylmethylamido bis(phenols) through peptide-catalyzed bromination: enantiodivergence as a consequence of a 2 amu alteration at an achiral residue within the catalyst. *J. Org. Chem.* ***82***, 11326–11336 (2017).

(*36*) A. T. Londregan, S. Jennings, L. Wei, General and mild preparation of 2-aminopyridines. *Org. Lett.* ***12***, 5254–5257 (2010).

(*37*) A. T. Londregan, S. Jennings, L. Wei, Mild addition of nucleophiles to pyridine *N*-oxides. *Org. Lett.* ***13***, 1840–1843 (2011).

(*38*) S. P. Clissold, E. M. Sorkin, K. L. Goa, Loratadine - a preliminary review of its pharmacodynamic properties and therapeutic efficacy" *Drugs* ***37***, 42–57 (1989).

(*39*) J. J. Piwinski, J. K. Wong, T. M. Chan, M. J. Green, A. K. Ganguly, Hydroxylated metabolites of loratadine: an example of conformational diastereomers due to atropisomerism. *J. Org. Chem.* ***55***, 3341–3350 (1990).

(*40*) B. Morgan, A. Zaks, D. R. Dodds, J. Liu, R. Jain, S. Megati, F. G. Njoroge, V. M. Girijavallabhan, Enzymatic kinetic resolution of piperidine atropisomers: synthesis of a key intermediate of the farnesyl protein transferase inhibitor, SCH66336. *J. Org. Chem.* ***65***, 5451–5459 (2000).

(*41*) J. Rouden, M. -C. Lasne, J. Blanchet, J. Baudoux, (–)-Cytisine and derivatives: synthesis, reactivity, and applications. *Chem. Rev.* ***114***, 712–778 (2014).

(*42*) J. W. Coe, P. R. Brooks, M. G. Vetelino, M. C. Wirtz, E. P. Arnold, J. Huang, S. B. Sands, T. I. Davis, L. A. Lebel, C. B. Fox, A. Shrikhande, J. H. Heym, E. Schaeffer, H. Rollema, Y. Lu, R. S. Mansbach, L. K. Chambers, C. C. Rovetti, D. W. Schulz, F. D. Tingley, B. T. O'Neill, Varenicline: an α4β2 nicotinic receptor partial agonist for smoking cessation. *J. Med. Chem.* ***48***, 3474–3477 (2005).

(*43*) G. R. Fulmer, A. J. M. Miller, N. H. Sherden, H. E. Gottlieb, A. Nudelman, B. M. Stoltz, J. E. Bercaw, K. I. Goldberg, NMR chemical shifts of trace impurities: common laboratory solvents, organics, and gases in deuterated solvents relevant to the organometallic chemist. *Organometallics* ***29***, 2176–2179 (2010).

(*44*) P. A. Lichtor, S. J. Miller, A one-bead-one-catalyst approach to aspartic acid-based oxidation catalyst discovery. *ACS Comb. Sci.* ***13***, 321–326 (2011).

(*45*) A. T. Londregan, S. Jennings, L. Wei, Mild addition of nucleophiles to pyridine *N*-oxides. *Org. Lett.* ***13***, 1840–1843 (2011).

(*46*) G. M. Sheldrick, A short history of SHELX. *Acta Cryst.* ***A64***, 112–122 (2008).

Acknowledgments: We thank Dr. Margaret J. Hilton for critical suggestions. We also would like to thank Dr. Brandon Q. Mercado for solving our X-ray crystal structures. **Funding:** This work is supported by the National Institute of General Medical Sciences of the National Institutes of Health for support (R35 GM132092). S.Y.H. is very grateful to the Swiss National Science Foundation for a postdoctoral fellowship. E.A.S. acknowledges the support of the NSF Graduate Research Fellowship Program. **Competing interests:** The authors declare that they have no competing interests. **Data and materials availability:** Experimental details and characterization data is available in the main text and/or the supplementary materials for all compounds. X-Ray crystallographic data for compounds **3l** (CCDC 1950272), **16** (CCDC 1950546), and **18** (CCDC 1950273) are available free of charge from the Cambridge Crystallographic Data Center.

Supplementary Materials:

Materials and Methods

Supplementary Text

Figures S1–S8

Tables S1–S3

References (*43–46*)

Figures

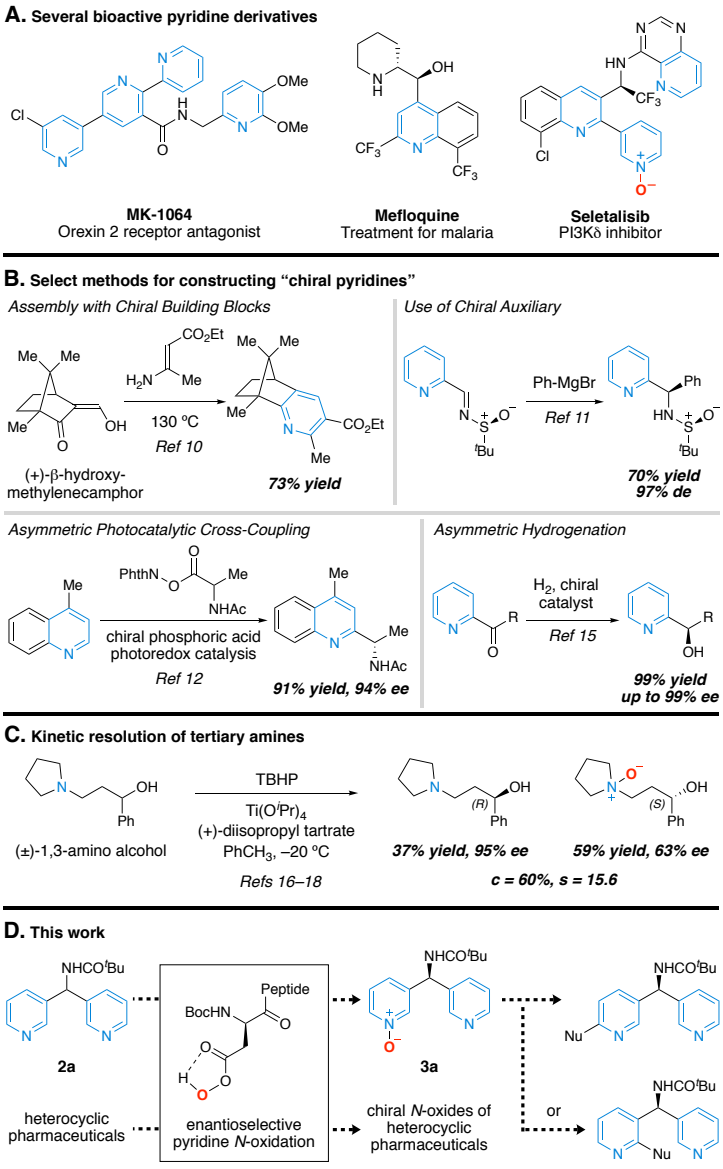

Fig 1. Examples of chiral *N*-heterocycles and methods for their construction. (**A**) Representative bioactive pyridine-containing compounds. (**B**) Several conventional strategies to access optically enriched pyridine-containing molecules. (**C**) Inspiration from enantioselective *N*-oxidation of tertiary amines. (**D**) The method reported herein for enantioselective *N*-oxidation of pyridines and heterocyclic pharmaceuticals. See supplementary materials for abbreviations.

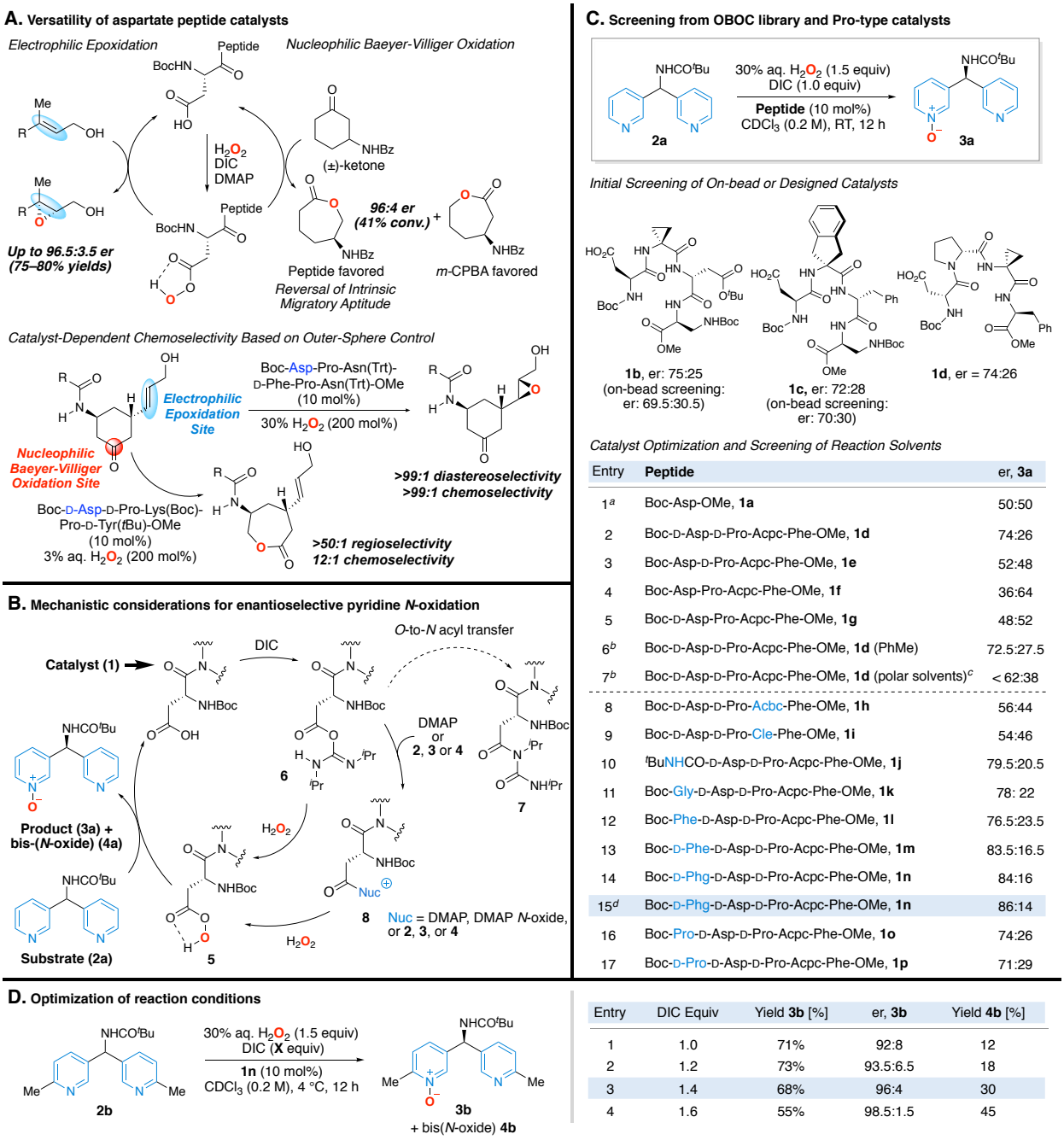

Catalyst Optimization and Screening of Reaction Solvents

Entry	Peptide	er, **3a**
1[a]	Boc-Asp-OMe, **1a**	50:50
2	Boc-D-Asp-D-Pro-Acpc-Phe-OMe, **1d**	74:26
3	Boc-Asp-D-Pro-Acpc-Phe-OMe, **1e**	52:48
4	Boc-Asp-Pro-Acpc-Phe-OMe, **1f**	36:64
5	Boc-D-Asp-Pro-Acpc-Phe-OMe, **1g**	48:52
6[b]	Boc-D-Asp-D-Pro-Acpc-Phe-OMe, **1d** (PhMe)	72.5:27.5
7[b]	Boc-D-Asp-D-Pro-Acpc-Phe-OMe, **1d** (polar solvents)[c]	< 62:38
8	Boc-D-Asp-D-Pro-Acbc-Phe-OMe, **1h**	56:44
9	Boc-D-Asp-D-Pro-Cle-Phe-OMe, **1i**	54:46
10	tBuNHCO-D-Asp-D-Pro-Acpc-Phe-OMe, **1j**	79.5:20.5
11	Boc-Gly-D-Asp-D-Pro-Acpc-Phe-OMe, **1k**	78: 22
12	Boc-Phe-D-Asp-D-Pro-Acpc-Phe-OMe, **1l**	76.5:23.5
13	Boc-D-Phe-D-Asp-D-Pro-Acpc-Phe-OMe, **1m**	83.5:16.5
14	Boc-D-Phg-D-Asp-D-Pro-Acpc-Phe-OMe, **1n**	84:16
15[d]	Boc-D-Phg-D-Asp-D-Pro-Acpc-Phe-OMe, **1n**	86:14
16	Boc-Pro-D-Asp-D-Pro-Acpc-Phe-OMe, **1o**	74:26
17	Boc-D-Pro-D-Asp-D-Pro-Acpc-Phe-OMe, **1p**	71:29

Entry	DIC Equiv	Yield **3b** [%]	er, **3b**	Yield **4b** [%]
1	1.0	71%	92:8	12
2	1.2	73%	93.5:6.5	18
3	1.4	68%	96:4	30
4	1.6	55%	98.5:1.5	45

Fig 2. Reaction development and catalyst optimization. (**A**) Previous applications of Asp-containing peptide catalysts. (**B**) Hypothesis of enantioselective *N*-oxidation of pyridine substrates. (**C**) Screening of peptide catalysts from one-bead-one-compound (OBOC) library and proline-type β-turn peptides. [a] The mono-*N*-oxide **2a** was produced in 63% yield. [b] Instead of $CDCl_3$, the solvent listed in parentheses was used in this reaction. [c] Polar solvents included: EtOAc, Et_2O, and THF. [d] The reaction was performed at 4 °C. Enantiomeric ratios were measured according to the eluent order. (**D**) Optimization of reaction conditions for pyridine *N*-oxidation with peptide **1n** performed on 0.05 mmol scale. See supplementary materials for abbreviations.

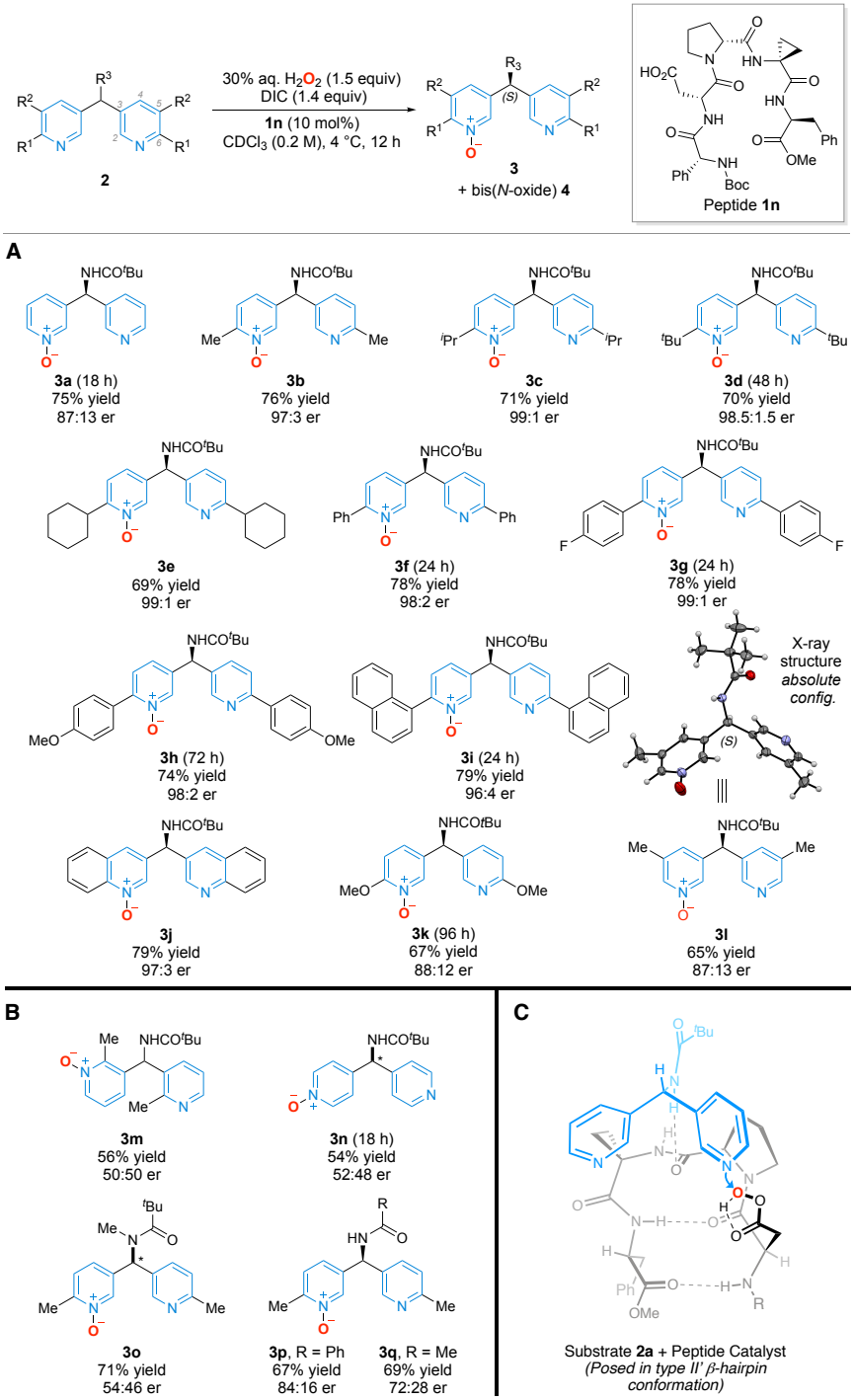

Fig 3. Substrate scope of the desymmetrization of bis(pyridine)s. (**A**) Substrates reacted well to excellently with peptide catalyst **1n**. (**B**) Substrates reacted with low to no selectivity. Different reaction times are noted in parentheses. For reaction details, see supplementary materials. (**C**) A speculative and heuristic model for the enantiomeric outcome. Absolute configuration of **3a**–**3k**, **3p**, **3q**, were determined by analogy to the single-crystal X-ray diffraction of **3l**, and the ones of **3m**–**3o** were listed as uncertain.

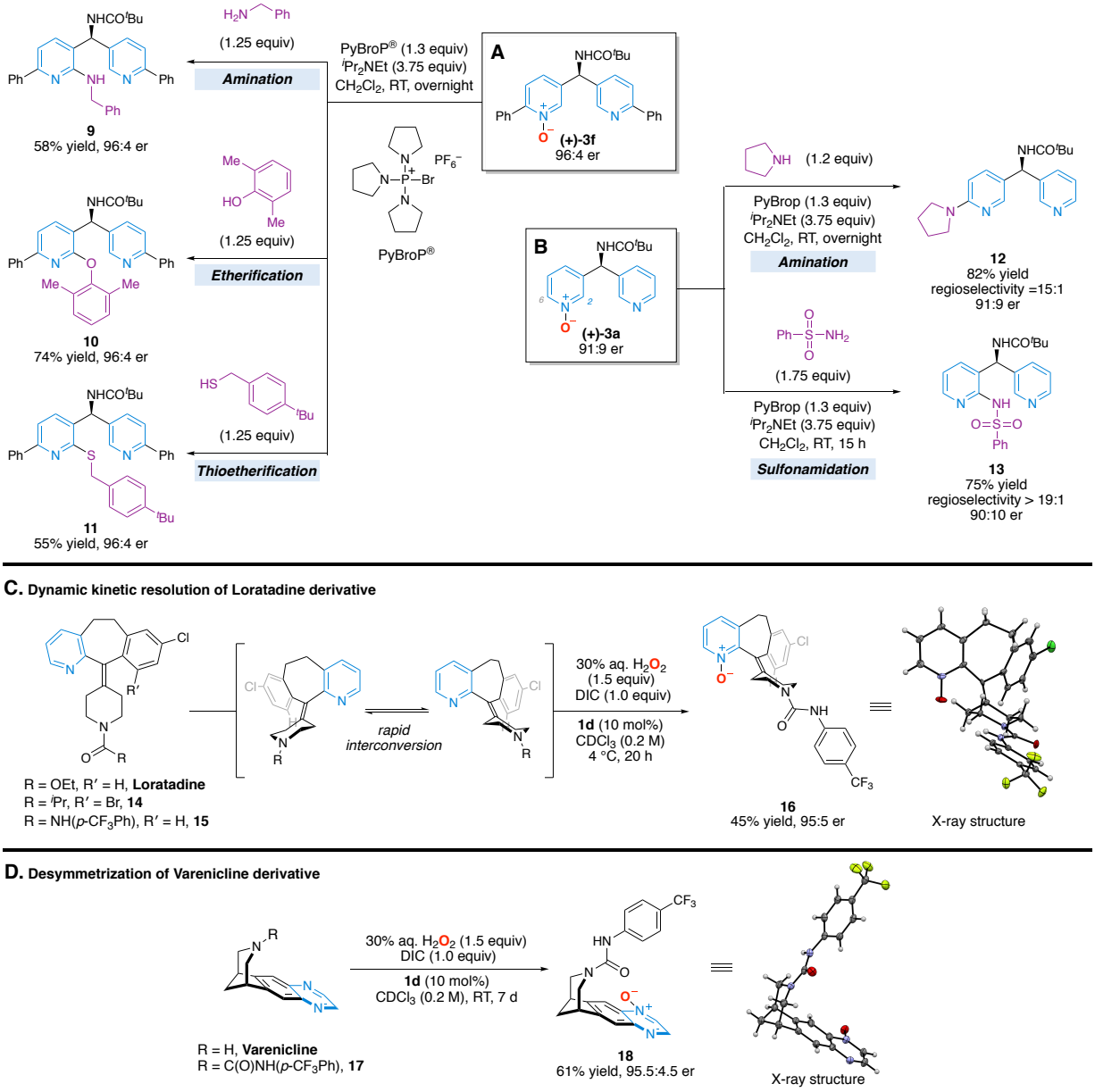

Fig 4. Derivatization and Applications. (**A**) Derivatization of enantioenriched **3f** *via* amination, etherification, and thioetherification. (**B**) Derivatization of enantioenriched **3a** through regioselective amination, arylation, and sulfonamidation. (**C**) Dynamic kinetic resolution of Loratadine derivative **15**. (**D**) Desymmetrization of Varenicline derivative **17**. See supplementary materials for abbreviations.